

Structure–function relationships in conjugated materials containing tunable thieno[3,4-*b*]pyrazine units

Michael E. Mulholland · Ryan L. Schwiderski ·
Seth C. Rasmussen

Received: 3 October 2011 / Revised: 4 January 2012 / Accepted: 13 February 2012 /
Published online: 26 February 2012
© Springer-Verlag 2012

Abstract A series of 2,3-difunctionalized 5,7-bis(2-thienyl)thieno[3,4-*b*]pyrazines containing electron-donating and electron-withdrawing side chains are reported to evaluate the potential tuning effect of the side chains on the electronic properties of these common terthienyl building blocks. In order to further study the resulting effects of such side chains in polymeric materials, the dihexyloxy-functionalized terthienyl was copolymerized with fluorene and its electronic properties compared with a number of analogous materials.

Keywords Conjugated polymers · Thieno[3,4-*b*]pyrazine · Structure–function relationships · Electronic tuning

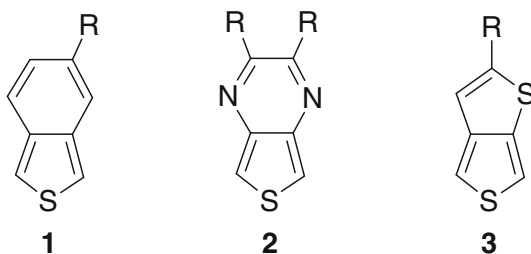
Introduction

One of the critical parameters of conjugated organic polymers is the band gap (E_g), which is the energetic separation between the material's filled valence and empty conduction bands [1–4]. As this corresponds to the HOMO–LUMO gap of the solid state material, the E_g determines such material properties as the lowest energy absorbance and the energy of any potential emission. Because of this, significant effort has been applied to developing methods for controlling the E_g of conjugated materials with the goal of producing technologically useful *reduced band gap* ($E_g = 1.5$ – 2.0 eV) and *low band gap* ($E_g < 1.5$ eV) polymers [4].

A number of approaches to reducing the E_g of conjugated materials have been reviewed, of which the most successful has been the application of fused-ring thiophenes [1–4]. This approach was first demonstrated by Wudl and coworkers in

M. E. Mulholland · R. L. Schwiderski · S. C. Rasmussen (✉)
Department of Chemistry and Biochemistry, North Dakota State University, NDSU Dept. 2735,
P.O. Box 6050, Fargo, ND 58108-6050, USA
e-mail: seth.rasmussen@ndsu.edu

Fig. 1 Fused-ring thiophene building blocks for the generation of low E_g materials



1984 [5, 6] with the polymerization of benzo[*c*]thiophene (**1**, R = H, Fig. 1). The motivation behind this approach was the idea that the fusion of a second aromatic ring to the *c*-face of the thiophene would enhance the quinoidal nature of the polymer backbone, thus resulting in significant reductions of the band gap [1–6]. Following the initial success of benzo[*c*]thiophenes, other fused-ring variants soon followed including thieno[3,4-*b*]pyrazines (TPs, **2**), and thieno[3,4-*b*]thiophenes (**3**) [1–4]. Thieno[3,4-*b*]pyrazines in particular have become quite popular building blocks and have been successfully applied to the generation of a wide range of both reduced band gap and low band gap conjugated materials [4].

The application of TPs is somewhat limited, however, as the majority of currently applied TPs consists of either the unfunctionalized parent or its dialkyl or diaryl analogues [7–10]. As a consequence, the limited variety of available functionality hinders the ability to tune the electronic and optical properties of the TP unit and the majority of any band gap tuning is derived from its copolymerization with other conjugated units [4]. To overcome this limitation, we have developed methods for the production of 2,3-dibromo- and 2,3-bis(bromomethyl)-TPs, through which a wide variety of previously unavailable TPs can be produced [9]. The ability to incorporate electron-donating and electron-withdrawing groups on the TPs now provides the potential for much more significant tuning of the resulting TP-based materials. Initial results from electropolymerized poly(thieno[3,4-*b*]pyrazine)s have demonstrated the ability to use the electronic nature of the side chains to tune the electronic properties of the resultant materials [11] and the current report aims to extend the study of potential side chain tuning to the commonly utilized TP-based terthienyl building blocks [4]. Side chain effects on a series of such terthienyls are reported and their application to TP-based copolymeric materials is investigated utilizing the well-studied poly[5,7-bis(2-thienyl)thieno[3,4-*b*]pyrazine-*co*-fluorene] framework (Fig. 2) [12–19].

Experimental

Materials and instrumentation

2,5-Bis(2-thienyl)-3,4-diaminothiophene (**5**) [20], 2,3-dibromothieno[3,4-*b*]pyrazine (**6**) [9], 2-(tributylstannyl)thiophene [20, 21], 2,3-dimethyl-5,7-bis(2-thienyl)thieno[3,4-*b*]pyrazine (**7**) [20, 21], and 2,7-dibromo-9,9-dioctyl-9*H*-fluorene (**8**)

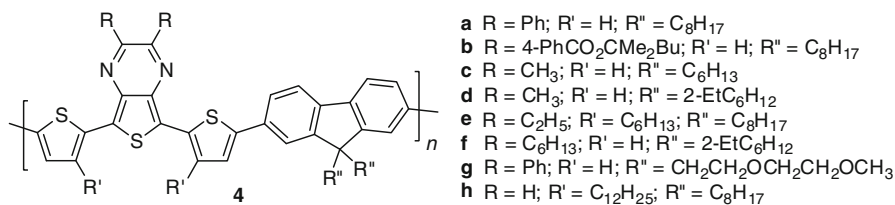


Fig. 2 Poly[5,7-bis(2-thienyl)thieno[3,4-*b*]pyrazine-*co*-fluorene]s

[22] were prepared as previously reported. THF was distilled from sodium benzophenone prior to use. CH₂Cl₂ was dried over CaH and distilled prior to use. DMF was dried over MgSO₄ prior to use. Chromatographic separations were performed using standard column methods with silica gel (230–400 mesh). Basic silica gel was prepared by pretreating the silica with 3% Et₃N in CH₂Cl₂. Unless otherwise stated, all other materials were reagent grade and used without further purification. All reactions were performed under a nitrogen atmosphere using oven-dried glassware. Melting points are corrected and were obtained using a heating block with a thermocouple connected to a digital thermometer. Unless otherwise stated, NMR spectra were obtained in CDCl₃ on a 400 MHz spectrometer and referenced to the chloroform signal. Electrochemical measurements were performed on an EC Epsilon potentiostat using a Pt disc working electrode and a Pt wire counter electrode. Solutions consisted of 0.1 M TBAPF₆ in CH₃CN and were sparged with argon for 20 min prior to data collection and blanketed with argon during the experiment. Terthiophene samples were measured as millimolar solutions and polymeric samples were measured as solid-state films drop-cast onto the Pt disc working electrodes. All potentials are referenced to a Ag/Ag⁺ reference (0.1 M AgNO₃/0.1 M TBAPF₆ in CH₃CN; 0.320 V vs. SCE) [23]. UV–Visible spectra were measured on a dual-beam scanning spectrophotometer using samples prepared as dilute solutions in 1-cm quartz cuvettes or thin films spun onto glass slides.

5,7-Bis(2-thienyl)-2,3-bis(bromomethyl)thieno[3,4-*b*]pyrazine (**9**)

Diamine **5** (1.39 g, 5.00 mmol) was added to absolute ethanol (80 mL), the mixture was heated with stirring until completely dissolved and allowed to cool to room temperature. 1,4-Dibromo-2,3-butanedione (1.89 g, 7.50 mmol) in 40 mL absolute ethanol was then added dropwise and the mixture was allowed to stir for 6 h. The mixture was then cooled to –25 °C, filtered, and washed with cold ethanol to give a purple solid (84–92% yield). ¹H NMR: δ 7.66 (dd, *J* = 3.6 Hz, 1.2 Hz, 2H), 7.39 (dd, *J* = 5.2 Hz, 0.8 Hz, 2H), 7.11 (dd, *J* = 5.2 Hz, 3.6 Hz, 2H). ¹³C NMR: δ 150.1, 137.5, 134.1, 127.7, 127.4, 126.3, 125.7, 31.6. HRMS *m/z* 506.8290 [M+Na]⁺ (calcd for C₁₆H₁₀Br₂N₂NaO₂S₃ 506.8265).

2,3-Bis(hexyloxymethyl)-5,7-bis(2-thienyl)thieno[3,4-*b*]pyrazine (**10**)

NaH (oil dispersion, 57% w/w, 0.40 g, 9.2 mmol) was washed with hexanes and then added to 1-hexanol (20 mL) and stirred overnight to ensure complete NaH

consumption. The hexanol solution was then added dropwise to **9** (0.486 g, 1.00 mmol) in 50 mL dry CH_2Cl_2 and the mixture allowed to stir for 6 h. Saturated aqueous NH_4Cl was then added, the CH_2Cl_2 removed by rotary evaporation, and the remaining aqueous hexanol solvent removed via vacuum distillation (45–50 °C at 15 mmHg). Water was then added and the mixture was extracted with CH_2Cl_2 . The combined organic fractions were dried with MgSO_4 , concentrated and purified by silica chromatography (50% CH_2Cl_2 /hexanes) to give a red–purple solid (50–60% yield). $^1\text{H NMR}$: δ 7.64 (dd, $J = 4$ Hz, 1.2 Hz, 2H), 7.36 (dd, $J = 4.8$ Hz, 1.2 Hz, 2H), 7.09 (dd, $J = 4.8$ Hz, 3.6 Hz, 2H), 4.86 (s, 4H), 3.62 (t, $J = 6.8$ Hz, 4H), 1.68 (p, $J = 6.8$ Hz, 4H), 1.39 (m, 4H), 1.30 (m, 8H), 0.89 (t, $J = 2.8$, 6H). $^{13}\text{C NMR}$: δ 152.4, 137.7, 134.6, 127.5, 126.7, 125.4, 125.0, 72.8, 71.6, 31.9, 30.0, 26.1, 22.8, 14.3. HRMS m/z 551.1846 $[\text{M}+\text{Na}]^+$ (calcd for $\text{C}_{28}\text{H}_{36}\text{N}_2\text{NaO}_2\text{S}_3$ 551.1831).

5,7-Bis(2-thienyl)-2,3-bis(*N,N*-diethylaminomethyl)thieno[3,4-*b*]pyrazine (**11**)

Diethylamine (25 mL, 242 mmol) was added dropwise to **9** (0.243 g, 0.500 mmol) in dry CH_2Cl_2 (25 mL) and the mixture was heated at reflux for 5 h. Water was then added and the mixture was extracted with CH_2Cl_2 (3×50 mL). The combined organic fractions were washed with saturated aqueous NaHCO_3 (2×100 mL) and brine (2×100 mL), dried with MgSO_4 , concentrated. The crude product was purified by basic silica chromatography (CH_2Cl_2) to give a dark red solid (60–98% yield). $^1\text{H NMR}$: δ 7.63 (dd, $J = 3.6$ Hz, 1.2 Hz, 2H), 7.36 (dd, $J = 5.2$ Hz, 1.2 Hz, 2H), 7.09 (dd, $J = 5.2$ Hz, 3.6 Hz, 2H), 4.10 (s, 4H), 2.73 (q, $J = 7.2$ Hz, 8H), 1.06 (t, $J = 7.2$ Hz 12H). $^{13}\text{C NMR}$: δ 154.6, 137.7, 135.0, 127.3, 126.5, 124.6, 124.5, 57.5, 46.6, 11.4. HRMS m/z 471.1707 $[\text{M}+\text{H}]^+$ (calcd for $\text{C}_{24}\text{H}_{31}\text{N}_4\text{S}_3$ 471.1705).

2,3-Dihexyloxythieno[3,4-*b*]pyrazine (**12**)

NaH (oil dispersion, 57% w/w, 1.00 g, 23.8 mmol) was washed with hexanes and then added to 60 mL DMF. 1-Hexanol (1.0 mL, 8.0 mmol) was added and the mixture stirred at room temperature for 5 min. Compound **6** (0.60 g, 2.0 mmol) was then added and the mixture was stirred for an additional 2 h. Aqueous NH_4Cl was added and the mixture was extracted with CH_2Cl_2 . The organic layer was dried with Na_2SO_4 , concentrated, and purified by silica chromatography (97:3, hexane:diethyl ether), giving a white solid (90–95% yield). mp 69.9–71.1 °C. $^1\text{H NMR}$: δ 7.36 (d, $J = 6.8$ Hz, 2H), 4.41 (t, $J = 6.8$ Hz, 2H), 1.85 (p, $J = 7.2$ Hz, 2H), 1.37 (m, 6H), 0.91 (t, $J = 2.4$ Hz, 3H). $^{13}\text{C NMR}$: δ 150.2, 138.3 112.4, 67.2, 31.6, 28.6, 25.8, 22.7, 14.1.

5,7-Dibromo-2,3-dihexyloxythieno[3,4-*b*]pyrazine (**13**)

A solution of **12** (0.38 g, 1.0 mmol) in 100 mL DMF was cooled to –78 °C. NBS (0.44 g, 2.5 mmol) was added, the reaction was warmed to –15 °C, and stirred for 3 h. The solution was poured into ice (100 mL) and stirred for 15 min to form a yellow solid. The solid was filtered, extracted in ether, and washed with 200 mL of water. The organic layer was collected, dried with MgSO_4 , concentrated, and

purified by silica chromatography (95:5, hexane:diethyl ether) to give a yellow solid (67% yield). mp 45.2–46.4 °C. ^1H NMR: δ 4.48 (t, $J = 6.8$ Hz, 2H), 1.86 (t, $J = 6.8$ Hz, 2H), 1.38 (m, 7H), 0.89 (t, $J = 2.4$ Hz, 3H); ^{13}C NMR: δ 151.1, 136.3, 98.8, 67.9, 31.6, 28.5, 25.8, 22.7, 14.1.

2,3-Dihexyloxy-5,7-bis(2-thienyl)thieno[3,4-*b*]pyrazine (**14**)

2-(Tributylstannyl)thiophene (0.39 g, 1.08 mmol) and **13** (0.21 g, 0.42 mmol) were combined in a 250 mL flask, evacuated, and backfilled with N_2 . Dry THF (100 mL) was then added by syringe, followed by a second N_2 cycling. $\text{PdCl}_2(\text{PPh}_3)_2$ (0.015 g, 0.02 mmol) was added, the solution heated to reflux, and stirred for 16 h. The solution was then allowed to cool to room temperature and solvent removed via rotary evaporation. The resulting material was dissolved in CH_2Cl_2 , washed with H_2O , dried with MgSO_4 , and concentrated via rotary evaporation. Purification was done by silica chromatography in (95:5, hexanes: CH_2Cl_2) yielding an orange solid (48% yield). ^1H NMR: δ 7.45 (dd, $J = 3.0, 1.2$ Hz, 2H), 7.31 (dd, $J = 4.5, 1.2$ Hz, 2H), 7.06 (dd, $J = 3.0, 4.5$ Hz, 2H), 4.55 (t, $J = 7.0$ Hz, 4H), 1.93 (t, $J = 7.0$ Hz, 4H), 1.52–1.38 (m, 12H), 0.94 (t, $J = 6.5$ Hz, 6H). ^{13}C NMR: δ 150.16, 135.40, 134.03, 127.04, 125.47, 123.29, 120.48, 68.08, 31.77, 28.52, 25.95, 22.80, 14.22.

2,3-Dihexyloxy-5,7-bis(5-trimethylstannyl-2-thienyl)thieno[3,4-*b*]pyrazine (**15**)

Dry hexanes (60 mL) was added via syringe to a flask containing **14** (0.06 g, 0.12 mmol) and the solution was cooled to 0 °C. TMEDA (0.05 mL, 0.35 mmol) was then added followed by BuLi (0.13 mL, 0.33 mmol) and the solution was stirred for 2 h. Me_3SnCl (0.3 mL, 0.33 mmol) was syringed into the solution and the reaction was allowed to stir overnight. The solution was poured over Et_3N -treated silica gel, filtered, and rinsed with 100 mL hexanes. The solution was concentrated via rotary evaporation to yield a yellow liquid (99%). ^1H NMR: δ 7.44 (d, $J = 3.2$, 2 H), 7.099 (d, $J = 1.6$, 2H), 4.40 (t, $J = 6.4$, 4H), 1.81 (m, $J = 6.8$, 4H), 1.53–1.20 (m, 16 H), 0.86 (t, $J = 6.8$, 6 H), 0.40 (s, 18H).

Poly[2,3-dihexyloxy-5,7-bis(2-thienyl)thieno[3,4-*b*]pyrazine-*co*-9,9-dioctyl-9H-fluorene] (**4i**)

Fluorene **8** (0.06 g, 0.12 mmol), **15** (0.10 g, 0.12 mmol), Pd_2dba_3 (0.002 g, 0.002 mmol), and $\text{P}(o\text{-tolyl})_3$ (0.02 g, 0.08 mmol) were combined in a flask. N_2 -purged toluene (15 mL) was then added by syringe and the solution evacuated and backfilled with N_2 . The reaction was then placed in an oil bath (95 °C) and allowed to react for 4 days. The reaction was then cooled, poured into 300 mL methanol, and filtered. The soluble fraction of polymer was collected in CHCl_3 and isolated by rotary evaporation. Further purification was accomplished by further washes with MeOH yielding a red solid (75%). ^1H NMR: δ 7.50 (m), 7.44 (m), 7.30 (m), 4.55 (br t), 1.92 (m), 1.6–0.6 (m). GPC: $M_w = 4000$, $M_n = 2700$, PDI = 1.48.

Results and discussion

The most prolific class of TP-based oligomers consists of terthienyls containing a central TP unit, the first examples of which were reported by Yamashita and co-workers in 1994 [20]. Such terthienyls are common precursors to TP-based copolymeric materials, resulting in a wide variety of materials with reported band gaps of 1.17–1.78 eV [4]. Many of these materials have also been utilized as donor materials for bulk heterojunction organic photovoltaic (OPV) devices.

To date, TP-based terthienyls are prepared in a method analogous to monomeric TPs via the double condensation of the diaminoterthiophene precursor **5** with the various α -diones to generate the central TP unit. These methods have been used to produce a wide variety of unfunctionalized-, dialkyl-, and diaryl-TP-based terthienyls [4], although with very little electronic variance. In attempts to extend the methods utilized for the production of monomeric 2,3-dibromo- and 2,3-bis(bromomethyl)-TPs to TP-based terthienyl analogues, it was found that 1,4-dibromo-2,3-butanedione can be easily condensed with **5** to generate the bis(bromomethyl) species **9** in high yield (Fig. 3). Various terthienyls can then be produced from intermediate **9** via simple substitution reactions as shown for the production of terthienyls **10** and **11**.

While the production of terthienyls from **9** is simple and straightforward, the α -methylene of the side chains reduces the potential electronic influence on the conjugated unit and the direct coupling of electron-donating or electron-withdrawing groups to the TP unit should result in a greater amount of electronic modulation. To accomplish the production of such terthienyls, substitution of dibromothieno[3,4-*b*]pyrazine **6** was accomplished as previously described [9] to generate the desired functionalized TP **12**, as shown in Fig. 3. Treatment with NBS then allowed simple bromination of the thiophene α -positions, followed by Stille coupling with stannylthiophene to generate the desired terthienyl **14**.

The electronic and optical data for a series of terthienyls are collected in Table 1 to illustrate the tuning effects of the TP functional groups in such terthienyl units. Previous studies on TPs have shown that the TP HOMO is predominately

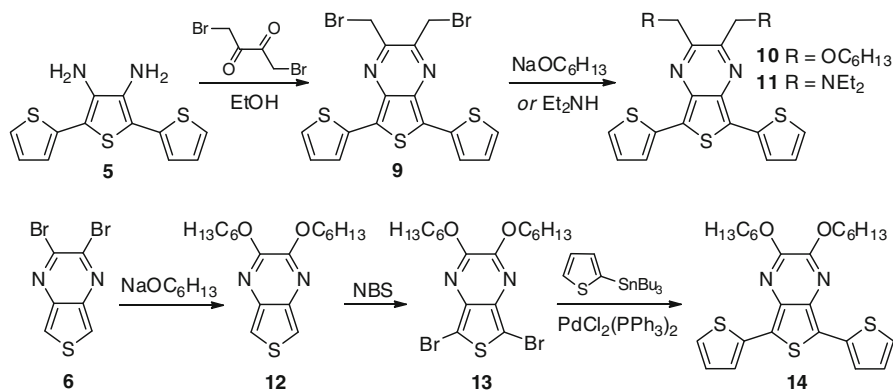


Fig. 3 Synthesis of the thieno[3,4-*b*]pyrazine-based terthienyl precursors

thiophene-localized while the LUMO is of greater pyrazine contribution [7–9]. As the HOMO and LUMO are localized on different portions of the TP species, the lowest energy transition in the UV–Vis spectrum is a broad charge transfer (CT) band, the energy of which can be modulated by the electronic effects of functional groups in the 2- and 3-positions [9]. Such functional groups are bound directly to the pyrazine ring, which contributes more significantly to the LUMO than the HOMO and therefore functional groups have a greater effect on the LUMO than the corresponding HOMO. Thus, electron-donating groups destabilize both the HOMO and the LUMO levels, while also increasing the corresponding HOMO–LUMO energy gap. In contrast, electron-withdrawing groups stabilize both the HOMO and the LUMO levels, while decreasing the HOMO–LUMO energy gap [9].

The addition of the 2-thienyl groups to the 5- and 7-positions of the TP unit results in an increase in conjugation and a HOMO which is now delocalized across the terthienyl backbone. As with monomeric TPs, the pyrazine ring here contributes little to the terthienyl HOMO, but contributes strongly to the LUMO. As a consequence, the effect of the side chains in the TP-based terthienyls is similar to that previously reported for the monomeric analogues [9], although with some significant differences. Thus, as shown in both Table 1 and the absorption spectra in Fig. 4, the HOMO–LUMO energy decreases as the electron-withdrawing nature of the side chain increases, resulting in a red-shift in the low-energy CT transition. Thus, replacing the strongly electron-donating hexyloxy groups to the mildly electron-withdrawing methylbromo groups result in a red-shift of over 100 nm.

Electrochemical characterization of the terthienyls by cyclic voltammetry (CV) allows a more detailed study of the electronic effects on the respective HOMO and LUMO levels. Typical of monomeric TPs, the TP-based terthienyls exhibit a well-defined irreversible oxidation assigned to the oxidation of the terthiophene backbone, as well as a quasireversible pyrazine-based reduction. The measured electrochemical potentials are provided in Table 1. As previously seen for monomeric TPs [9], the potential of oxidation becomes more positive as the

Table 1 Optical and electrochemical data for theino[3,4-*b*]pyrazine-based terthienyls

Terthienyl	R	λ_{\max} (nm) ^a	E_{pa} (V, oxidation) ^b	$E_{1/2}$ (V, reduction) ^b	E_{HOMO}^c	E_{LUMO}^f
14	OC ₆ H ₁₃	440	0.45	−2.03 ^d	−5.43	−3.23
7	CH ₃	492	0.50	−1.68	−5.49	−3.51
11	CH ₂ NEt ₂	511	0.32 ^c , 0.62	−1.65	−5.15	−3.54
10	CH ₂ OC ₆ H ₁₃	511	0.57	−1.48	−5.53	−3.62
9	CH ₂ Br	547	0.62	−1.26	−5.55	−4.15

^a In CH₃CN

^b 0.10 M Bu₄NPF₆ in CH₃CN; potential versus Ag/Ag⁺. E_{pa} is the anodic peak potential. $E_{1/2}$ is the half-wave potential

^c Nitrogen-based oxidation

^d E_{pc}

^e $E_{\text{HOMO}} = -(E_{[\text{onset,ox vs. Fc+}/\text{Fc}]} + 5.1)$ (eV), Ref. [24]

^f $E_{\text{LUMO}} = -(E_{[\text{onset,red vs. Fc+}/\text{Fc}]} + 5.1)$ (eV), Ref. [24]

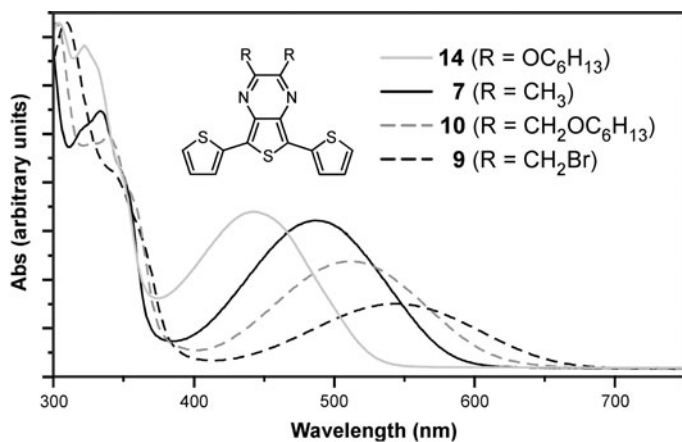


Fig. 4 UV-Visible spectra of a series of thieno[3,4-*b*]pyrazine-based terthienyls

electron-withdrawing nature of the side chain is increased, indicative of a stabilization of the HOMO. An important difference, however, is that this effect is significantly attenuated in the terthienyl series. Thus, the change in potential of oxidation from the hexyloxy to methylbromo functional groups is nearly 300 mV in the monomeric TPs [9], but only 170 mV in the terthienyl series is reported here. This difference is due to the fact that the effect of the two additional 2-thienyl groups in the terthienyls contributes more significantly to the HOMO, resulting in a much greater effect on the HOMO energy, as illustrated by a shift in the potential of oxidation by 850 mV from monomeric TP to terthienyl [7, 9]. Thus, the destabilization of the HOMO by the added external thiophenes effectively overpowers the weaker contribution of the TP side chains.

In contrast, the addition of the external thiophenes contribute much less to the terthienyl LUMO and only results in a slight stabilization of the LUMO levels as illustrated by the slightly lower reduction potentials of the terthienyls in comparison to the monomeric TP analogues [9]. As the pyrazine contributes most significantly to the LUMO, the TP functional groups provide the greatest effect on the LUMO energies, as illustrated by the nearly 800 mV shift in the corresponding reduction potentials. Thus, the large red shifts in the energy of the CT transitions discussed above are primarily due to stabilization of the LUMO energy levels through the use of electron-withdrawing side chains.

To further evaluate the effect of the TP side chains in a copolymeric material, the hexyloxy-functionalized terthienyl **14** was converted to the corresponding trimethylstannyl analogue and copolymerized with dibromofluorene via Stille coupling to give polymer **4i**, as detailed in Fig. 5. The poly[5,7-bis(2-thienyl)thieno[3,4-*b*]pyrazine-*co*-fluorene] framework was chosen here as it is perhaps the most well-studied of the various TP-based terthienyl copolymeric materials [12–19]. As a result, there are thus a number of analogous materials available in the literature for easy comparison.

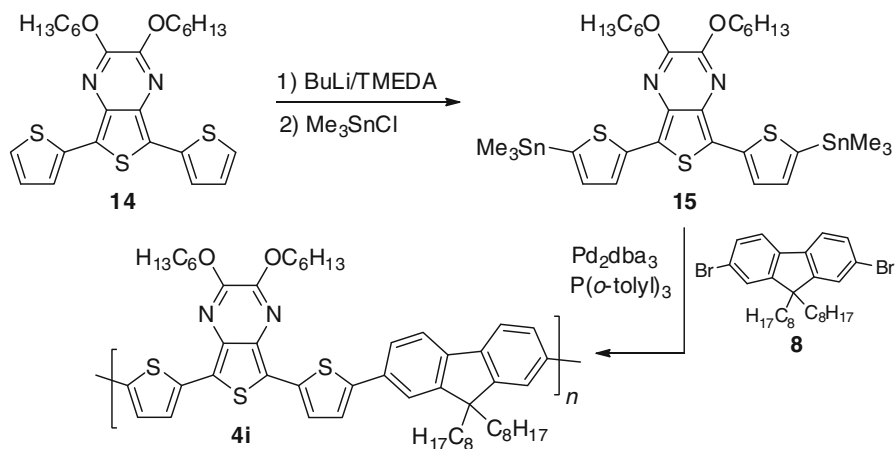


Fig. 5 Synthesis of poly[2,3-dihexyloxy-5,7-bis(2-thienyl)thieno[3,4-*b*]pyrazine-*co*-9,9-dioctyl-9H-fluorene]

Table 2 Electric data for poly[5,7-bis(2-thienyl)thieno[3,4-*b*]pyrazine-*co*-fluorene]s

Polymer	R	λ_{\max} (film, nm)	E_g^{opt} (eV)	E_{HOMO}^a	E_{LUMO}^b	Reference
4i	OC ₆ H ₁₃	350, 400, 440 (sh)	2.25	−5.3	−3.2	This study
4a	Ph	616	1.61	−5.2	−3.7	[12–14]
4d	CH ₃	600	1.61	−5.6	−3.8	[18]
4h	H	667	1.60	−5.7	−3.6	[15]
4b	<i>p</i> -PhCO ₂ R ⁺	710	1.37	nr	nr	[17]

nr not reported

^a $E_{\text{HOMO}} = -(E_{[\text{onset,ox vs. Fc+}/\text{Fc}]} + 5.1)$ (eV), Ref. [24]

^b $E_{\text{LUMO}} = -(E_{[\text{onset,red vs. Fc+}/\text{Fc}]} + 5.1)$ (eV), Ref. [24]

The electronic properties of **4i** and various previously reported analogues are given in Table 2. The thin film absorption spectrum of a **4i** is shown in Fig. 6. For the most part, the majority of reported materials with this copolymeric framework are reduced band gap polymers with band gaps near 1.6 eV [4]. As expected from the previous trends both in the monomeric TPs and in the TP-based terthienyls above, the shift to alkoxy side chains results in destabilization of both the HOMO and LUMO. In addition, this results in a corresponding increase in the material band gap, with a band gap now above 2 eV.

Interestingly, Helgesen and Krebs [17] reported polymer **4b** that incorporates phenylester side chains on the TP unit. While these phenylesters were applied as thermocleavable side chains and not as a means to tune the polymer electronic properties, the significantly electron-withdrawing nature of the side chains resulted in a reduction of the band gap. As a consequence of the side chain applied, a polymeric framework normally resulting in reduced band gap materials can generate a true low band gap system with an E_g of 1.37 eV. While the electrochemistry was

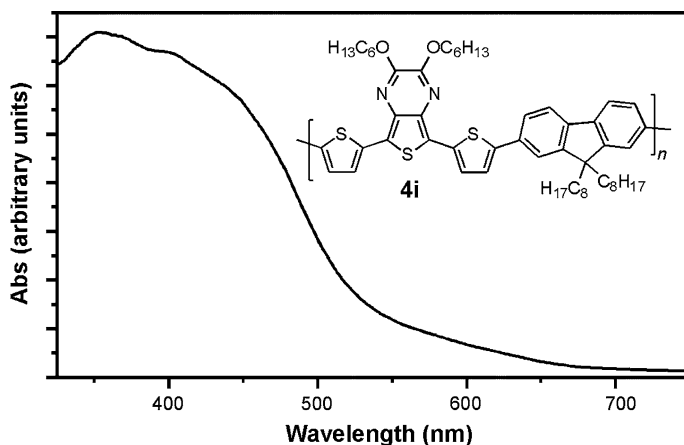


Fig. 6 Absorption spectrum of a thin film of copolymer **4i**

not reported, it would be expected from the trends above that this also resulted in stabilization of both the HOMO and the LUMO of the material.

The results above illustrate that the ability to incorporate either electron-withdrawing or electron-donating groups into the 2- and 3-positions of TPs allows the direct tuning of the electronic properties of TP-based materials. In the application to copolymeric materials, the effect of the side chains on the HOMO is diminished, but largely determines the LUMO energy and as a result the material's band gap as well. The ability to modulate the properties of materials via TP functional groups would allow one to forgo the more complex tuning approaches of recent efforts and provide means for the production of systems that are much more structurally and synthetically simple. This would also provide the potential to achieve the desired electronic and optical properties for various device applications while holding the backbone structure constant and thus resulting in reduced morphological changes from material to material.

Acknowledgments The authors wish to thank the National Science Foundation (DMR-0907043) and North Dakota State University for support of this research.

References

1. Roncali J (1997) Synthetic principles for bandgap control in linear π -conjugated systems. *Chem Rev* 97:173–205
2. Rasmussen SC, Pomerantz M (2007) Low band gap conducting polymers, chapter 12. In: Skotheim TA, Reynolds JR (eds) *Handbook of conducting polymers*, vol 1, 3rd edn. CRC Press, Boca Raton
3. Rasmussen SC, Ogawa K, Rothstein SD (2008) Synthetic approaches to band gap control in conjugated polymeric materials, chapter 1. In: Nalwa HS (ed) *Handbook of organic electronics and photonics*, vol 1. American Scientific Publishers, Stevenson Ranch
4. Rasmussen SC, Schwiderski RL, Mulholland ME (2011) Thieno[3,4-*b*]pyrazines and their applications to low band gap organic materials. *Chem Commun* 47:11394–11410

5. Wudl F, Kobayashi M, Heeger AJ (1984) Poly(isothianaphthene). *J Org Chem* 49:3382–3384
6. Kobayashi M, Colaneri N, Boysel M, Wudl F, Heeger AJ (1985) The electronic and electrochemical properties of poly(isothianaphthene). *J Chem Phys* 82:5717–5723
7. Kenning DD, Mitchell KA, Calhoun TR, Funfar MR, Sattler DJ, Rasmussen SC (2002) Thieno[3,4-*b*]pyrazines: synthesis, structure, and reactivity. *J Org Chem* 67:9073–9076
8. Rasmussen SC, Sattler DJ, Mitchell KA, Maxwell J (2004) Photophysical characterization of 2,3-difunctionalized thieno[3,4-*b*]pyrazines. *J Lumin* 190:111–119
9. Wen L, Nietfeld JP, Amb CM, Rasmussen SC (2008) Synthesis and characterization of new 2,3-disubstituted thieno[3,4-*b*]pyrazines: tunable building blocks for low band gap conjugated materials. *J Org Chem* 73:8529–8536
10. Rasmussen SC, Mulholland ME, Schwiderski RL, Larsen CA (2011) Thieno[3,4-*b*]pyrazines and its extended analogues: important building blocks for conjugated materials. *J Heterocycl Chem* 48. doi: [10.1002/jhet.1051](https://doi.org/10.1002/jhet.1051)
11. Wen L, Nietfeld JP, Amb CM, Rasmussen SC (2009) New tunable thieno[3,4-*b*]pyrazine-based materials. *Synth Met* 159:2299–2301
12. Perzon E, Wang X, Zhang F, Mammo W, Delgado JL, de la Cruz P, Inganas O, Langa F, Andersson MR (2005) Design, synthesis and properties of low band gap polyfluorenes for photovoltaic devices. *Synth Met* 154:53–56
13. Zhang F, Perzon E, Wang X, Mammo W, Andersson MR, Inganas O (2005) Polymer solar cells based on a low-bandgap fluorene copolymer and a fullerene derivative with photocurrent extended to 850 nm. *Adv Funct Mater* 15:745–750
14. Admassie S, Inganas O, Mammo W, Perzon E, Andersson MR (2006) Electrochemical and optical studies of the band gaps of alternating polyfluorene copolymers. *Synth Met* 156:614–623
15. Zhu Y, Champion RD, Jenekhe SA (2006) Conjugated donor-acceptor copolymer semiconductors with large intramolecular charge transfer: synthesis, optical properties, electrochemistry, and field effect carrier mobility of thienopyrazine-based copolymers. *Macromolecules* 39:8712–8719
16. Lee W, Cheng K, Wang T, Chueh C, Chen W, Tuan C, Lin J (2007) Effects of acceptors on the electronic and optoelectronic properties of fluorene-based donor–acceptor–donor copolymers. *Macromol Chem Phys* 208:1919–1927
17. Helgesen M, Krebs FC (2010) Photovoltaic performance of polymers based on dithienylthienopyrazines bearing thermocleavable benzoate esters. *Macromolecules* 43:1253–1260
18. Zhou E, Cong J, Yamakawa S, Wei Q, Nakamura M, Tajima K, Yang C, Hashimoto K (2010) Synthesis of thieno[3,4-*b*]pyrazine-based and 2,1,3-benzothiadiazole-based donor-acceptor copolymers and their application in photovoltaic devices. *Macromolecules* 43:2873–2879
19. Chao C-Y, Lim H, Chao C-H (2010) Molecular engineering of conjugated copolymers for photoactive layer in polymer solar cells. *Polym Prepr* 51(1):715–716
20. Kitamura C, Tanaka S, Yamashita Y (1994) Synthesis of new narrow bandgap polymers based on 5,7-di(2-thienyl)thieno[3,4-*b*]pyrazine and its derivatives. *J Chem Soc Chem Commun* 1585–1586
21. Kitamura C, Tanaka S, Yamashita Y (1996) Design of narrow-bandgap polymers. Syntheses and properties of monomers and polymers containing aromatic-donor and o-quinoid-acceptor units. *Chem Mater* 8:570–578
22. Cho SY, Grimsdale AC, Jones DJ, Watkins SE, Holmes AB (2007) Polyfluorenes without mono-alkylfluorene defects. *J Am Chem Soc* 129:11910–11911
23. Larson RC, Iwamoto RT, Adams RN (1961) Reference electrodes for voltammetry in acetonitrile. *Anal Chim Acta* 25:371–374
24. Cardona CM, Li W, Kaifer AE, Stockdale D, Bazan GC (2011) Electrochemical considerations for determining absolute frontier orbital energy levels of conjugated polymers for solar cell applications. *Adv Mater* 23:2367–2371